RSC Advances

This is an *Accepted Manuscript*, which has been through the Royal Society of Chemistry peer review process and has been accepted for publication.

Accepted Manuscripts are published online shortly after acceptance, before technical editing, formatting and proof reading. Using this free service, authors can make their results available to the community, in citable form, before we publish the edited article. This *Accepted Manuscript* will be replaced by the edited, formatted and paginated article as soon as this is available.

You can find more information about *Accepted Manuscripts* in the Information for Authors.

Please note that technical editing may introduce minor changes to the text and/or graphics, which may alter content. The journal's standard Terms & Conditions and the Ethical guidelines still apply. In no event shall the Royal Society of Chemistry be held responsible for any errors or omissions in this *Accepted Manuscript* or any consequences arising from the use of any information it contains.

ROYAL SOCIETY OF CHEMISTRY

www.rsc.org/advances

Characterization of Polymer/Epoxy Buried Interfaces with Silane Adhesion Promoters before and after Hygrothermal Aging for the Elucidation of Molecular Level Details Relevant to Adhesion

Nathan Ulrich[a], John Myers[a], Zhan Chen[a,*]

[a]Department of Chemistry, University of Michigan, 930 North University Avenue, Ann Arbor, Michigan 48109, United States

*Correspondence to: Zhan Chen (zhanc@umich.edu), Tel: 734-615-4189

RSC Advances Accepted Manuscript

Abstract:

Buried interfacial structures containing epoxy underfills are incredibly important in the microelectronics industry and their structures determine the interfacial adhesion properties and ultimately their lifetime. Delamination at such interfaces leads to premature failure of microelectronic devices. In this work, the intrinsically surface sensitive technique, sum frequency generation (SFG) vibrational spectroscopy, was utilized to investigate the molecular structure of buried epoxy interfaces before and after accelerated stress testing in order to relate the molecular-level structural changes to the macroscopic adhesion strength and determine what effect silane adhesion promoters have on polymer/epoxy systems. Strongly hydrogen bonded water was detected at hydrophilic epoxy interfaces and this was correlated with a large decrease in adhesion strength. The addition of a small amount of adhesion promoters drastically improved the adhesion strength following accelerated stress testing at a relatively hydrophilic polymer/epoxy interface, and they were also capable of preventing interfacial water. A hydrophobic polymer/epoxy interface was also studied and silane adhesion promoters were found to improve the adhesion strength following stress testing of the hydrophobic interface as well. This research demonstrates that molecular structural studies of buried epoxy interfaces during hygrothermal aging using SFG vibrational spectroscopy can greatly contribute to the overall understanding of moisture-induced failure mechanisms of organic adhesives found in microelectronic packaging.

Introduction:

In recent decades, the microelectronics industry has evolved rapidly with innovations such as the integrated circuit (IC), which revolutionized the field. IC technology was dramatically changed with the advent of the flip-chip, which decreased the size of the IC and increased the speed.[1, 2] In

RSC Advances Accepted Manuscript

flip-chip assemblies, a solder bump replaces the wire necessary (common in earlier predecessors) for older microchips, which is currently the most space-efficient method for connecting an IC to a microchip. This new technology enables the flip-chip device to have an incredibly small footprint in the electronic device.[3] When flip-chips were initially designed, ceramic substrates were utilized and there were not issues with differences in the thermal expansion coefficients (TEC). Now organic substrates such as poly(ethylene terephthalate) (PET) and polyimide are being utilized, there are issues with TEC mismatch, which generates thermal stress and can cause premature failure in the electronic devices.[4]

Underfill envelopment is utilized in conjunction with flip chip dies in order to laminate substrates, which distributes and minimizes the solder joint stress and strains, which then improves the devices capability to withstand thermal cycling fatigue testing.[5] The most common type of epoxy utilized is the bisphenol-type[6] complemented with silane molecules, which have been shown to greatly increase the adhesion strength.[7]

Delamination, where the die and the substrate become completely separated, is of great interest to the microelectronic industry, as it can cause premature failure;[8] however, this can be mitigated by utilizing an underfill with a low Young's modulus.[9] Delamination of underfill at the interface can drastically reduce solder joint reliability, and allow moisture to accumulate at interfaces, which may cause additional failure modes.[10] Thermal stress can promote delamination at the underfill/chip, and the solder/underfill interfaces,[11] which means thermoconductive epoxy underfills are necessary for long-term reliability and are an effective method for controlling heat dissipation.[12] It is widely accepted that interfacial failures can be caused by interfacial peeling

RSC Advances Accepted Manuscript

and delamination.[13] Any delaminations that occur at the underfill/die interface will propagate to the neighboring solder bumps and lead to solder joint fatigue and failure. The onset and propagation of delaminations in flip chip assemblies exposed to thermal cycling are governed by the cyclic stresses and damage occurring at the underfill/die interface. For this reason, underfills are improved by increasing the strength of adhesion, the resistance to aging, and interfacial resilience.[5] It is worth mentioning that to better mitigate the thermal stress, thermally conductive epoxies that are capable of quickly dissipating heat have been utilized,[3] and this technique can increase the lifetime of the flip-chip by 20 times.[14] However, this method has not been widely used yet.

One method of characterizing the resilience of an epoxy underfill is to perform hygrothermal aging and then analyze the samples to see how they change in the presence of stress. Hygrothermal treatments are performed by exposing the samples to high heat and humidity, which can decrease the strength of adhesion,[15] by disrupting the interfacial van der Waals interactions.[16] The bulk of the research on epoxy underfills for microelectronic packaging has focused on bulk and surface analysis *ex situ*. Techniques such as adhesion strength testing,[17] scanning acoustic microscopy (SAM),[18] thermogravimetric analysis,[19] moiré interferometry,[20] Fourier transform infrared spectroscopy (FTIR),[15] scanning electron microscopy (SEM),[15, 19] and X-ray photoelectron spectroscopy (XPS)[18] have all been utilized to investigate epoxy underfills and determine how they behave in the presence of hygrothermal treatment. Techniques such as, SAM, moiré interferometry, SEM, and XPS, can provide structural information or elemental analysis, but they cannot provide chemical or interfacial functional group orientation information. Delamination can be monitored by techniques such as SAM, but this technique is

RSC Advances Accepted Manuscript

incapable of determining molecular-level interactions relevant to adhesion, which are primarily determined by the interactions and the structures of the molecules at the interface.[21] One substantial issue with all of these methods is that none of them are capable at looking at the molecular-level detail *in situ* at the buried interface, which is relevant where the die is connected to a substrate via an underfill. Buried interfaces provide a substantial challenge for researchers due to a lack of techniques available that can probe these regions and provide chemical information. Buried interfaces have been traditionally studied by separating the two substrates, characterizing the resulting surfaces, and then attempting to extrapolate the molecular structure at the buried interface from the *ex situ* measurements on the two exposed surfaces. The problem with this method is that the molecular interactions that may determine the strength of adhesion at the interface may be destroyed when the substrates are separated and analyzed, thus no measurement is made while the system is in its native state. In order to fully elucidate how hygrothermal testing affects delamination of epoxy underfills at buried interfaces, a technique must be utilized that can provide chemical specific information, and make *in situ* measurements, nondestructively.

Over the past few years, SFG vibrational spectroscopy has been used extensively as a noninvasive analytical tool capable of studying buried interfaces and surfaces, and generating molecular-level detail *in situ*.[22,23] SFG vibrational spectroscopy is a nonlinear optical technique capable of probing any interface that is accessible to laser light. SFG spectroscopy can be utilized to investigate surface and interfacial chemical structure, such as coverage, orientation, and orientation distribution of interfacial functional groups. It can probe interfacial molecular interactions, such as interfacial diffusion and interfacial hydrogen bonding networks.[24,25] This

RSC Advances Accepted Manuscript

technique has also been extensively utilized to study polymers systems and buried polymer interfaces.[26,27,28-30,31,32] Research in our group also focuses on SFG spectroscopy in order to assess model epoxies systems typically used as underfill material in the microelectronics.[33-42] SFG has also probed fundamental interactions relevant in adhesion, such as H-bonding,[24] acid-base interactions,[43] and diffusion.[25] In addition, SFG spectroscopy has investigated the structure of interfacial water,[44] which is useful for investigating hygrothermal treatment of buried interfaces. In our research group we have extensively studied epoxy systems with SFG spectroscopy, we have shown how this technique can investigate the structure-function relationship of complex systems.[33,34, 35,45,46,37,47-49]

Particularly, we investigated interactions between polymers and silane adhesion promoters at buried polymer interfaces using SFG in situ. We demonstrated that hydrogen bonds can be formed between polymer surface (e.g., C=O groups on PET surface) and silane molecules (e,g., silane NH_2 end groups).[24] Such hydrogen bonds can play an important role in adhesion. It was also found that both the silane epoxide groups and the silane amine groups can diffuse into the polymer films and dissolve or modify the polymer films at interfaces,[47] which can affect adhesion.

We also investigated the effects of hygrothermal treatment on polymer interfacial structure and adhesion. Our research was focused on the buried interface between polymer and epoxy.[34] It was found that after hygrothermal treatment water had migrated to the interface, detected by SFG spectroscopy, and the macroscopic properties had drastically changed and the adhesion strength was greatly reduced.

RSC Advances Accepted Manuscript

In this study, SFG spectroscopy was employed to investigate how epoxy interfaces behave in the presence of high temperature and humidity and to determine if silane adhesion promoters can prevent or delay the effects of hygrothermal aging. Specifically, we studied the deuterated polystyrene (dPS)/epoxy, and deuterated poly(ethylene terephthalate) (dPET)/epoxy buried interfaces with and without silane adhesions promoters before and after hygrothermal aging. The deuterated polymers were used in this study to avoid spectral confusion between the polymer and the epoxy (with or without silanes added). The polymer poly (ethylene terephthalate) (PET) is an excellent model for poly (butylene terephthalate), which is ubiquitous in the microelectronics industry.[50] The polymer polystyrene (PS) serves as a model for a hydrophobic polymer at an interface, so we can compare and contrast the hygrothermal effect on both a hydrophobic and relatively hydrophilic interface. The epoxy under investigation is a proprietary commercial adhesive/potting compound, which is primarily composed of BADGE and polyoxypropylenediamine, but also contains many other components including catalysts, so it is a sufficient model epoxy system for our purpose. Even though there is no silica present in the epoxy, we believe that the fundamental interfacial chemistry of this material is representative of underfill components commonly utilized in the microelectronics industry.

SFG and attenuated total internal reflectance-Fourier transform infrared spectroscopy (ATR-FTIR) spectra of these interfaces were collected before and after hygrothermal aging in order to elucidate the interfacial molecular structure and provide a possible mechanism for adhesion loss. The distinct difference between this research and our previous hygrothermal study[34] is that in this research, we introduced silane adhesion promoters to the epoxy material. In addition to the control systems (without added silanes), three different silane adhesion promoters were utilized:

RSC Advances Accepted Manuscript

(3-aminopropyl)-trimethoxysilane (ATMS), (3-glycidoxypropyl) trimethoxysilane (GPS), and octadecyltrimethoxysilane (OTMS), to determine what affect the promoters have and if they can prevent some water uptake at the interface. All three silanes have the same head-group, trimethoxy silane, with different terminal chains. The methoxy head group can be replaced with a hydroxyl group through a hydrolysis reaction and then further react with either the polymer or the epoxy matrix (e.g., with epoxy glycidyl groups). For the end groups, the amine or the epoxide group on ATMS and GPS, respectively, are highly reactive. The amine groups can react with epoxy epoxide groups, while the GPS epoxide groups can react with the cross linking agents in the epoxy. The methyl and methylene groups on OTMS are much more inert.

Lap shear adhesion tests were performed on the same systems for SFG studies to correlate macroscopic adhesion changes during hygrothermal aging to changes observed in the spectral data, in order to understand the structure-function relationship of the buried epoxy interfaces and to understand adhesion on a more fundamental level. The success of such investigations will ultimately lead to more robust underfills that can withstand greater stress.

Experimental:

Materials.

Right angle fused silica prism substrates (Altos Photonics, Inc., Bozeman, MT) were utilized for all SFG experiments as solid supports for polymer thin film deposition. The polymer PET, with a deuterated aliphatic chain (d4-PET or dPET), and deuterated polystyrene (d8-PS or dPS) were both purchased from Polymer Science, Inc., Monticello, IN. Two solutions (2.0 weight %) were made by dissolving dPET in 2-chlorophenol (Sigma-Aldrich, St. Louis, MO, >99%) and dPS in chloroform (Sigma-Aldrich, St. Louis, MO, >99.8%). Three different silanes were utilized: (3-

RSC Advances Accepted Manuscript

glycidoxypropyl) trimethoxysilane (GPS), (3-Aminopropyl)-trimethoxysilane (ATMS), and octadecyltrimethoxysilane (OTMS), were all purchased from Sigma-Aldrich (St. Louis, MO) and 1.5 weight % of each silane was added to an epoxy sample prior to curing. Commercial epoxy resin 3302 (CE3302) was obtained from Epoxies Etc., Cranston, RI. CE3302 base is a proprietary blend, composed predominantly of bisphenol A-(epichlorohydrin) and trace amounts of bis(1,2,2,6,6-pentamethyl-4 piperidinyl)-sebacate and 4-nonylphenol. The CE3302 hardener used was poly(oxypropylenediamine). Bisphenol A digylcidyl ether (BADGE) is produced in the curing process and then reacts further with poly(oxypropylenediamine) to produce a cross-linked structure.[35] All chemical structures can be found in Figure 1.

Sample Preparation

Silica prisms were cleaned first in a concentrated sulfuric acid bath saturated with potassium dichromate followed by a rinse of deionized water and then they were finally dried under a stream of nitrogen. Following the acid cleaning, the substrates were exposed to air plasma (PE-50, Plasma Etch) for 2 minutes prior to polymer film deposition. Polymer solutions were spin-cast on the fused silica substrates at 2500 rpm for 30 s using a P-6000 spin coater (Speedline Technologies). In order to remove solvent residue, the samples were covered and placed overnight in the fume hood. For epoxy curing, the mixing ratio for resin to hardener was 2:1 by mass. After vigorously mixing the resin and hardener together, the epoxy was cured on top of the spin-cast polymer films according to manufacturer specifications (2 hours at 52°C).[35] After epoxy curing, the samples were exposed to 85°C and 100% relative humidity (RH) environmental conditions for defined periods of time by placing the samples above liquid water in a home-built container. The container is not completely sealed. There is a cover on top of the container, so the pressure inside the container should be very close to atmospheric pressure. The

RSC Advances Accepted Manuscript

pressure was not rigorously controlled, but it was constant for all samples. Right angle silicon prisms were used in all ATR-FTIR experiments as solid supports. Silicon substrates were cleaned and samples prepared using the same methods for the silica samples.

SFG and ATR-FTIR

SFG is a second-order nonlinear optical process, which probes the second order nonlinear susceptibility of the material. The selection rules provide SFG spectroscopy with submonolayer surface and interface sensitivity,[51-53] which make SFG spectroscopy a versatile and unique instrumentation capable of investigating interfacial systems. In a typical SFG system, the visible and mid-infrared (IR) input beams overlap upon an interface spatially and temporally. In our SFG experiments, both input beams were 20 Hz and contained 20 ps pulses and the pulse energies of the visible and IR beams are 30 μJ and 100 μJ, respectively. The SFG signal is generated at the sample interface and collected by a monochromator along with a gated photomultiplier tube (PMT). The monochromator can be tuned automatically while scanning the IR beam frequency. All SFG spectra in this experiment were collected using the ssp (s-polarized sum frequency output, s-polarized visible input, and p-polarized IR input) polarization combination. SFG spectra were collected from the buried interface between the polymer and after curing, after 24 hours hygrothermal treatment, and after 48 hours hygrothermal treatment. Because the aliphatic group deuterated PET and deuterated PS were used in this study, no aliphatic C−H signals were generated from the polymer at the buried polymer/substrate interface (in the spectral region scanned). The use of prism substrates and the adoption of the experimental geometry shown in Figure 2 greatly enhanced SFG signals compared to the use of the previous experimental geometry utilizing window substrates.[37, 39, 54] The SFG spectra collected from solid/solid buried interfaces are very weak. We repeated each experiment at least four times and

RSC Advances Accepted Manuscript

for each time, at least four samples were prepared. The results are reproducible and each spectrum presented in this work is the average of many SFG spectra. ATR-FTIR measurements were performed using a Nicolet 6700 FT-IR spectrometer controlled by OMNIC software. The input angle was approximately 45°. Single-bounce ATR-FTIR measurements with a silicon prism internal reflection element as a solid support was utilized due to its spectral transparency in the 2500−3500 cm^{-1} region (Figure 2).

Lap Shear Adhesion Test.

Adhesion lap shear tests were performed at room temperature after the specified hygrothermal aging time using a method based on ASTM D3163 (Figure 2). After the sheets were completely separated, an abrupt drop in adhesion strength was observed. The maximum adhesion strength observed before the sudden drop in force was utilized for all reported adhesion strength measurements. All adhesion failures were primarily adhesive failure at the interface as determined by a visual comparison of the delaminated area and a control region that was not exposed to epoxy adhesive, which shows that the interfacial molecular structures reported are related to the interfacial adhesive properties. The adherends that were utilized were made of nondeuterated PS or PET. The dimensions of the adherents were 5.0 x 3.0 x 0.5 cm and the bonded region was 0.5 x 3.0 x 0.2 cm. All results are the average of 3 or more samples being tested.

Results and Discussion:

Interface between dPET and Commercial Epoxy

RSC Advances Accepted Manuscript

In order to fully understand the control dPET/epoxy interface, the first system that was investigated is this control sample, with no additional silane adhesion promoters added to the commercial epoxy. There is one weak peak present in the SFG spectrum collected from the dPET/epoxy control prior to hygrothermal aging at 2960 cm^{-1}, which can be assigned to the antisymmetric stretching of the epoxy methyl group (Figure 3: a1). After 24 hours of hygrothermal treatment, an additional peak at 3150 cm^{-1} was observed, which can be assigned to interfacial water O-H stretching. It is worth mentioning that the 3150 cm^{-1} signal is contributed by strongly hydrogen bonded water. After 48 hours of hygrothermal treatment, the same two peaks were present, but the water peak grew in intensity relative to the methyl peak. The three spectra were fit and it was found that the 2960 cm^{-1} signal shifts by 10 cm^{-1} to 2970 cm^{-1} following the first hygrothermal treatment. This should be due to the change of the interfacial environment after hygrothermal aging. We believe that this is evidence that the interfacial region greatly changes after hygrothermal aging. The selection rules of SFG determine that SFG can only detect ordered water at the interface. Here ordered water was detected in the SFG spectra, which shows the water molecules migrated to the interface, strongly hydrogen bonded, and adopted some ordering. The peak around 3150 cm^{-1} is quite broad and this is due to the hydrogen bonding that occurs in water. Water molecules can have different hydrogen bonding environments. Since there is water detected after hygrothermal treatment at the interface, we believe that the adhesion strength will decrease, which we show below.

To understand how silane adhesion promoters affect water uptake, dPET/epoxy interfaces in the presence of the three silane adhesion promoters, ATMS, GPS, and OTMS, mixed into the epoxy (Figure 3: a2, a3, and a4, respectively) were investigated. For the ATMS and GPS systems, no

RSC Advances Accepted Manuscript

SFG signal was detected before or after hygrothermal aging, showing that the system is disordered at the interface and remains disordered at the interface throughout the aging process, which means water vapor is not moving to the interface and forming an ordered structure through a H-bonding network. This shows that ATMS and GPS are capable of preventing structural changes and ordered water uptake at the interface. As we indicated above, only 1.5 % of the silane was added to the epoxy bulk. Here it is clearly shown that a small amount of the silane in the epoxy bulk can greatly vary the interfacial structure between the polymer and epoxy. As we reported before,[35] the absence of the SFG signal from the polymer/epoxy (with silane) interface is likely due to the interfacial diffusion, and such interfacial diffusion may enhance the interfacial adhesion. We believe that after adding ATMS or GPS, they can segregate to the interface and diffuse through the interface. Therefore we believe that the adhesion at such interfaces should be relatively stronger, which will be further discussed below. For the OTMS system, the methyl group symmetric stretch and Fermi resonance are present in the SFG spectra throughout the aging process and no interfacial water is detected, however the two peaks change in intensity relative to each other. Such methyl signals can be contributed from both epoxy and OTMS. This study shows that with only 1.5 % OTMS molecules in the epoxy bulk, they are capable of preventing interfacial water, but the methyl groups are still reorienting during the aging process, indicated by the peak ratio changing. In the past, we demonstrated that the interfacial methyl groups detected by SFG may be related to weak adhesion, which will be discussed further below while we present the adhesion testing data. In summary, here SFG studies clearly show that the small amount of silane added to epoxy can effectively minimize/reduce the interfacial ordered water layer formation.

RSC Advances Accepted Manuscript

To see if water can move into the dPET/epoxy system, a supplementary technique was utilized, ATR-FTIR. The theoretical penetration depth of the evanescent wave was calculated as 800 nm, the dPET thin-film is approximately 100 nm, which means this technique can probe 700 nm into the epoxy region (this region, relative to SFG, is considered to be the bulk).[34] In all three spectra (pretreatment, 24 hours, 48 hours hygrothermal aging) for each of the four systems (control, ATMS, GPS, and OTMS), there are three peaks present in the C-H stretching frequency region (Figure 3: b1, b2, b3, and b4) at 2870, 2930, and 2965 cm^{-1}, which can be assigned to the epoxy methyl symmetric stretch, methylene antisymmetric stretch, and methyl antisymmetric stretch, respectively.[55] Since ATR-FTIR detects signals from the bulk material, and we only added 1.5 % of silanes to the epoxy bulk, we therefore believe that these signals are dominated by the contributions from the epoxy. Subsequent to the 24 hour hygrothermal aging there was a new peak that emerged at 3400 cm^{-1}, which can be assigned to O–H stretch of water from the bulk region of the epoxy. This signal is contributed by the weakly hydrogen bonded water molecules. After 48 hours, the water absorbance peak grew in intensity relative to the 24 hour spectrum, indicating that water continued to diffuse into the epoxy bulk with increased aging. One difference observed in the ATR-FTIR spectral data is the OTMS system, Figure 3 b4, which has an additional peak at 2850 cm^{-1} following hygrothermal treatment that can be assigned to the methylene symmetric stretch. Also the methylene antisymmetric stretching signal increased. This could be due to the OTMS being less reactive with the epoxy and migrating to the interface more after the hygrothermal treatment, being detected in the ATR-FTIR spectrum.

In order to correlate the molecular-level detail to the macroscopic properties, lap shear adhesion testing was performed before and after 24 hours of hygrothermal aging, see Figure 4. For all four

RSC Advances Accepted Manuscript

systems, there was a decrease in adhesion strength after hygrothermal treatment. The adhesion decrease was reported for underfills at 100% R.H previously.[56] Here, the control system had the biggest drop in adhesion, going from 8.1 MPa to 1.9 MPa, a decrease of 76%. For the adhesion promoters, ATMS had the smallest decrease, from 10.6 MPa to 7.5 MPa (decrease of 29%), followed by GPS, from 8.2 MPa to 5.4 MPa (decrease of 34%), and the largest decrease in adhesion strength for the promoters was OTMS, which went from 7.7 MPa to 4.3 MPa (decrease of 44%). For all three silanes added, the adhesion after hygrothermal aging is more than twice of the control. These results show that silane adhesion promoters have the ability to prevent some loss in adhesion strength after hygrothermal aging.

Figure 3b shows similar ATR-FTIR spectra for different samples under similar condition, but adhesion-testing results indicated that they have very different adhesion strength. This shows that the interfacial structure plays an important role in adhesion. PET is a relatively polar polymer, which means it is energetically favorable for water to form a hydrogen-bonding structure at the interface, and this is what is seen in the SFG spectrum for the control system. After hygrothermal aging, there is a peak assigned to water, which shows that water can migrate to the interface and form bonding interactions with the polymer. For the control system, there is water detected at both the interface and bulk, which is what one would expect considering the fact that no adhesion promoters were added. The lap shear results show a big decrease in adhesion for the control and a smaller decrease for the systems with silane adhesion promoters. This shows that if there is ordered water (and bulk water) detected, the adhesion strength will be drastically reduced (decrease of 71% for the control).

RSC Advances Accepted Manuscript

In contrast from the control sample, all the SFG spectra collected from the interfaces between PET and epoxy with silane added do not exhibit substantial water contribution. As we discussed previously,[35] if all variables remain constant, ordered methyl groups at an interface should yield lower adhesion strength. The control and OTMS systems have ordered methyl groups, from the SFG spectra, and the adhesion strength of these systems is lower than the ATMS and GPS systems, which have disordered interfaces in contact with epoxy and higher adhesion strength. The Control system had higher adhesion strength, before aging, than OTMS, which is predicted due to the stronger signal in the SFG spectrum from OTMS, showing that the methyl groups are more ordered than the control. For the systems with silane adhesion promoters there is no water detected at the interface, which indicates that water was not able to form an ordered structure. The dPET/epoxy systems with GPS, ATMS, and OTMS have been investigated previously (without hygrothermal aging) and the spectra presented in this work match the literature, with no signal coming from the GPS and ATMS systems and strong signal coming from the OTMS system.[35] This shows that the adhesion promoters are capable of preventing water migration to the interface.

The promoters ATMS and GPS are good at reducing water because the amine in ATMS and the epoxide ring in GPS can further react with the epoxy matrix once they migrate to the interface and become chemically immobilized, which then prevents the water molecules from becoming ordered because the water molecules cannot form an ordered structure. The OTMS promoter makes the interface more nonpolar, but it cannot react further with the epoxy matrix, so it decreases the water uptake but it does not increase the level of adhesion strength by reacting further. Thus, the OTMS prevents loss of adhesion strength due to the prevention of interfacial

RSC Advances Accepted Manuscript

ordered water formation, but it does not increase the adhesion strength by reacting further with the epoxy matrix like the reactions ATMS and GPS are capable of undergoing. It was found in a previous investigation,[35] that ordered methyl groups at the interface lead to weaker adhesion than disordered methyl groups, which is one reason why both the control and OTMS have lower adhesion than the ATMS and GPS samples. Even though SFG spectra from the interfaces between PET and epoxy with ATMS or GPS are similar after hygrothermal treatment, adhesion strengths decreased substantially, which may be due to the effect of bulk water in epoxy detected by ATR-FTIR.

Interface between dPS and Commercial Epoxy

As we discussed above, PET has a relative hydrophilic surface compared to many other polymers. In order to see if a more hydrophobic interface behaves differently from PET (dPET/epoxy), the dPS/epoxy interface was investigated. The effects of hygrothermal aging was examined by collecting the SFG spectrum from the dPS/epoxy interface, see Figure 5: a1. There are two peaks present in the SFG spectrum of dPS/epoxy control prior to hygrothermal aging at 2870 cm^{-1} and 2940 cm^{-1}, which can be assigned to the epoxy methyl group symmetric stretching and the Fermi resonance of the epoxy methyl group. After 24 hours and 48 hours of hygrothermal treatment the peak ratios in the spectra fluctuate slightly, but there is no interfacial water detected. We believe that this is evidence that the interfacial region does not change greatly after hygrothermal aging. Ordered water was not detected, which shows the water molecules are not capable of forming ordered structures at this hydrophobic interface.

RSC Advances Accepted Manuscript

To see if silane adhesion promoters can change how water responds at a hydrophobic interface, the same three silane adhesion promoters were added to the dPS/epoxy system (Figure 5: a2, a3, and a4). For all three silane promoter systems, there are two peaks present in the SFG spectrum at 2870 cm^{-1} and 2940 cm^{-1}, which can be assign to the symmetric stretching and the Fermi resonance of the epoxy methyl group, respectively. No substantial changes were observed in the spectra throughout hygrothermal aging.

To confirm that water can move into the bulk of the dPS/epoxy systems, ATR-FTIR was used again to study all dPS/epoxy systems. In all three spectra (pretreatment, 24 hours, 48 hours hygrothermal aging) for each of the three systems including the control, ATMS, and GPS systems, there are three peaks present in the C-H stretching frequency region (Figure 5: b1, b2, and b3, respectively) at 2870, 2930, and 2965 cm^{-1}, which can be assigned to the epoxy methyl symmetric stretch, methylene antisymmetric stretch, and methyl antisymmetric stretch, respectively.[55] Differently, Figure 5: b4 shows strong signals at 2870 and 2930 cm^{-1}, contributed by methylene symmetric and antisymmetric stretches. Similar to our explanation for Figure 3: b4, this could be due to the OTMS being less reactive with the epoxy and migrating to the interface more. Subsequent to the 24 hour hygrothermal aging there was a new peak that emerged centered at 3400 cm^{-1}, which can be assigned to O–H stretch of water from the bulk region of the epoxy. After 48 hours the water absorbance peak grew in intensity relative to the 24 hour spectrum, indicating that water continued to diffuse into the epoxy bulk with increased aging.

RSC Advances Accepted Manuscript

Lap shear adhesion testing was performed for the dPS/epoxy systems before and after 24 hour hygrothermal aging, see Figure 6. For all four systems there was some decrease in the level of adhesion strength. The control system went from 7.4 MPa to 3.0 MPa (decrease of 59%). For the adhesion promoters, ATMS had the smallest decrease, from 8.7 MPa to 4.4 MPa (decrease of 50%), followed by GPS, from 8.2 MPa to 3.7 MPa (decrease of 55%), and the largest decrease in adhesion strength was OTMS, which went from 7.6 MPa to 2.7 MPa (decrease of 64%). These results show that ATMS and GPS have the ability to prevent some loss of adhesion strength after hygrothermal aging, while OTMS actually makes the decrease in adhesion strength larger.

The polymer PS is a relatively nonpolar one, which means water cannot form an H–bonding structure at the interface easily, and this is what is seen in the SFG spectrum for the control system, and no ordered water is detected. For the systems there is no water detected by SFG, which indicates that no ordered water is present in the sample. This shows that the control and all three adhesion promoters are capable of preventing water ordering at the interface. We see in the ATR-FTIR spectra that there is water present in the bulk, even though no water is detected at the interface with SFG. The lap shear results show the measured adhesion strengths for all the samples decrease, showing that the water in the bulk may play an important role in adhesion reduction for the PS system. The interfaces between dPS and epoxy with added ATMS and GPS have less adhesion reduction, because the amine in ATMS and the epoxide ring in GPS can further react with the epoxy in the bulk as well as at the interface once they migrate to the interface. For the control sample and the sample with OTMS, the adhesion decreases are larger. For OTMS, it was found in a previous investigation,[35] that it is energetically favorable for it to segregate to the interface and order, leading to weaker adhesion. It is interesting to see in the

RSC Advances Accepted Manuscript

ATR-FTIR spectra, all the spectra are similar except those from the dPS/epoxy interface with OTMS before and after 24 hours hygrothermal treatment, therefore the signals seen in the spectrum originate from OTMS molecules, which are clearly seen, showing that they can segregate to the interfacial region (800 nm range from the interface).

Conclusions and Outlook:

In this study, molecular structures at buried epoxy interfaces were investigated *in situ* during before and after hygrothermal aging using SFG and ATR-FTIR. As we reported previously[35] and repeated in this work, the dPET control prior to aging has higher adhesion strength than the dPS system, and the SFG spectra show that the dPS system has more ordered methyl groups, because the peak intensity is greater in the dPS/epoxy spectra than the dPET/epoxy spectra. However, after the hygrothermal treatment, the dPS/epoxy has stronger adhesion. This is because PET is more hydrophilic, and an ordered water layer can be formed at the interface, reducing adhesion. In contrast, dPS is more hydrophobic, therefore it is more difficult for water to segregate to the dPS/epoxy interface to reduce adhesion.

In this research, for the dPET/epoxy interface, we added three different silanes to the epoxy. Even though the silane amount added is very small, all three silane adhesion promoters were capable of preventing interfacial changes throughout hygrothermal aging. No order was detected in ATMS and GPS samples, but the OTMS sample was well ordered. The adhesion loss was observed to be much smaller compared to the control sample.

RSC Advances Accepted Manuscript

For all four dPS/epoxy samples, there were no substantial changes detected throughout hygrothermal aging. This lack of changing could be due to the hydrophobic property of dPS, which prevents water from forming an ordered layer at the interface. There was bulk water detected in all eight systems, which shows how silane adhesion promoters are not capable of preventing the bulk water absorption.

For the dPET/epoxy systems the control had the biggest decrease in adhesion strength after aging, while ATMS and GPS had the smallest change, potentially due to their ability to react further once they have migrated to the interface, while OTMS did not increase the adhesion strength after testing, which could be due to its inability to undergo further reactions at the interface. For the dPS/epoxy systems, the highest adhesion strength after aging was the ATMS and GPS systems, while the control and OTMS had the lowest adhesion strength.

From this work it is clear that relatively hydrophilic surfaces can have initial higher adhesion, but through hygrothermal aging the strength of the adhesion is drastically reduced, but this can be mitigated by using a silane adhesion promoter that is capable of undergoing further reactions at the interface or in the bulk. The hydrophobic polymer has lower adhesion strength prior to hygrothermal treatment, but can handle the treatment better than its hydrophilic counterpart. The adhesion promoters can be utilized to increase the strength of adhesion and reduce adhesion loss after hygrothermal treatment of PS, but the effects are not as substantial as the PET. This is the first study, to our knowledge, that investigates polymer – epoxy (containing silane) interactions in the presence of high humidity and temperature at the molecular level. Understanding the mechanism of hygrothermal aging affects the molecular structure and orientation at buried

RSC Advances Accepted Manuscript

interfaces *in situ* will contribute to the understanding of moisture-induced failure mechanisms in microelectronic packages and help facilitate better design and development of more robust underfills that can withstand greater stress testing compared to their predecessors.

Acknowledgement
This work is supported by the Semiconductor Research Corporation (SRC contract no. 2012-KJ-2282).

RSC Advances Accepted Manuscript

Reference

1. H.-M. Tong, *Mater. Chem. Phys.*, 1995, **40**, 147-161.
2. C. P. Wong, *Mater. Chem. Phys.*, 1995, **42**, 25-30.
3. *The United States of America Pat.,* 1998.
4. M.-L. Sham and J.-K. Kim, *J. Electron. Packag.*, 2005, **127**, 47-51.
5. M. K. Rahim, J. C. Suhling, R. C. Jaeger and P. Lall, 2005.
6. S. Luo, T. Yamashita and C. P. Wong, *J. Electron. Manuf.*, 2000, **10**, 191-200.
7. K. C. Yung and H. Liem, *J. Appl. Polym. Sci.*, 2007, **106**, 3587-3591.
8. Y. L. Zhang, D. X. Q. Shi and W. Zhou, *Microelectron. Reliab.*, 2006, **46**, 409-420.
9. S. Rzepka, M. A. Korhonen, E. Meusel and C. Y. Li, *J. Electron. Packaging*, 1998, **120**, 342-348.
10. X. J. Fan, H. B. Wang and T. B. Lim, *IEEE Trans. Compon. Packag. Manuf. Technol.*, 2001, **24**, 84-91.
11. T. K. Lee and T. B. Lim, *Electronics Packaging Technology Conference, 1998. Proceedings of 2nd*, **1998**, DOI: 10.1109/EPTC.1998.756015, 274-278.
12. S. Jie, H. Fatima, A. Koudymov, A. Chitnis, X. Hu, H. M. Wang, J. Zhang, G. Simin, J. Yang and M. Asif Khan, *IEEE Electron. Device Lett.*, 2003, **24**, 375-377.
13. Z. Q. Jiang, Y. Huang and A. Chandra, *J. Electron. Packaging*, 1997, **119**, 127-132.
14. S. Hegde, R. Pucha and S. Sitaraman, *J. Mater. Sci. Mater. Electron.*, 2004, **15**, 287-296.
15. W. K. Chiang, Y. C. Chan, B. Ralph and A. Holland, *Int. J. Adhes. Adhes.*, 2008, **28**, 109-119.
16. B. M. Sharratt, L. C. Wang and R. H. Dauskardt, *Acta Materialia*, 2007, **55**, 3601-3609.
17. S. Luo and C. P. Wong, *IEEE Trans. Compon. Packag. Technol.*, 2005, **28**, 88-94.
18. K.-W. G. Lee, M. A.; Duchesne, E, *Electron. Mater. Lett.*, 2006, **2**, 171-174.
19. L. K. Teh, M. Teo, E. Anto, C. C. Wong, S. G. Mhaisalkar, P. S. Teo and E. H. Wong, *IEEE Compon. Packag. Technol.*, 2005, **28**, 506-516.
20. P. Jin-Hyoung, J. Kyung-Woon, P. Kyung-Wook and L. Soon-Bok, *IEEE Trans. Compon. Packag. Technol.*, 2010, **33**, 215-221.
21. F. Awaja, M. Gilbert, G. Kelly, B. Fox and P. J. Pigram, *Prog. Polym. Sci.*, **2009**, **34**, 948-968.
22. O. Mermut, D. C. Phillips, R. L. York, K. R. McCrea, R. S. Ward and G. A. Somorjai, *J. Am. Chem. Soc.*, 2006, **128**, 3598-3607.
23. I. V. Stiopkin, H. D. Jayathilake, A. N. Bordenyuk and A. V. Benderskii, *J. Am. Chem. Soc.*, 2008, **130**, 2271-2275.
24. C. L. Loch, D. Ahn, C. Chen, J. Wang and Z. Chen, *Langmuir*, 2004, **20**, 5467-5473.
25. Chen, J. Wang, C. L. Loch, D. Ahn and Z. ChenChen, *J. Am. Chem. Soc.*, 2004, **126**, 1174-1179.
26. X. Lu, M. L. Clarke, D. Li, X. Wang, G. Xue and Z. Chen, *J. Phys. Chem. C*, 2011, **115**, 13759-13767.
27. S. J. Kweskin, K. Komvopoulos and G. A. Somorjai, *Appl. Phys. Lett.*, 2006, **88**, 134105.
28. G. P. Harp, H. Rangwalla, M. S. Yeganeh and A. Dhinojwala, *J. Am. Chem. Soc.*, 2003, **125**, 11283-11290.
29. M. Xiao, X. Zhang, Z. J. Bryan, J. Jasensky, A. J. McNeil and Z. Chen, *Langmuir*, 2015, **31**, 5050-5056.

RSC Advances Accepted Manuscript

30. Q. Li, R. Hua and K. C. Chou, *J. Phys. Chem. B*, 2008, **112**, 2315-2318.
31. S. J. Kweskin, K. Komvopoulos and G. A. Somorjai, *Langmuir*, 2005, **21**, 3647-3652.
32. H. Ye, A. Abu-Akeel, J. Huang, H. E. Katz and D. H. Gracias, *J. Am. Chem. Soc.*, 2006, **128**, 6528-6529.
33. A. V. Vázquez, B. Holden, C. Kristalyn, M. Fuller, B. Wilkerson and Z. Chen, *ACS Appl. Mater. Interfaces*, 2011, **3**, 1640-1651.
34. J. N. Myers, C. Zhang, K.-W. Lee, J. Williamson and Z. Chen, *Langmuir*, 2014, **30**, 165-171.
35. C. Zhang, J. Hankett and Z. Chen, *ACS Appl. Mater. Interfaces*, 2012, **4**, 3730-3737.
36. Z. Chen, *Prog. Polym. Sci.*, 2010, **35**, 1376-1402.
37. C. Zhang, N. E. Shephard, S. M. Rhodes and Z. Chen, *Langmuir*, 2012, **28**, 6052-6059.
38. A. V. Vázquez, A. P. Boughton, N. E. Shephard, S. M. Rhodes and Z. Chen, *ACS Appl. Mater. Interfaces*, 2010, **2**, 96-103.
39. A. V. Vázquez, N. E. Shephard, C. L. Steinecker, D. Ahn, S. Spanninga and Z. Chen, *J. Colloid Interface Sci.*, 2009, **331**, 408-416.
40. C. L. Loch, D. Ahn, A. V. Vázquez and Z. Chen, *J. Colloid Interface Sci.*, 2007, **308**, 170-175.
41. C. L. Loch, D. Ahn and Z. Chen, *The Journal of Physical Chemistry B*, 2006, **110**, 914-918.
42. C. L. Loch, D. Ahn, C. Chen and Z. Chen, *The Journal of Adhesion*, 2005, **81**, 319-345.
43. A. Kurian, S. Prasad and A. Dhinojwala, *Langmuir*, 2010, **26**, 17804-17807.
44. K. Nanjundiah, P. Y. Hsu and A. Dhinojwala, *J. Chem. Phys.*, 2009, **130**.
45. X. Lu, J. Han, N. Shephard, S. Rhodes, A. D. Martin, D. Li, G. Xue and Z. Chen, *J. Phys. Chem. B*, 2009, **113**, 12944-12951.
46. J. N. Myers and Z. Chen, *Chin. Chem. Lett.*, 2015, DOI: 10.1016/j.cclet.2015.01.016, 1-6.
47. C. Zhang, J. N. Myers and Z. Chen, *Langmuir*, 2014, **30**, 12541-12550.
48. S. Ye, S. Morita, G. Li, H. Noda, M. Tanaka, K. Uosaki and M. Osawa, *Macromolecules*, 2003, **36**, 5694-5703.
49. P. L. Hayes, A. R. Keeley and F. M. Geiger, *The Journal of Physical Chemistry B*, 2010, **114**, 4495-4502.
50. J. Che, B. Luan, X. Yang, L. Lu and X. Wang, *Materials Letters*, 2005, **59**, 1603-1609.
51. a. J. Moad and G. J. Simpson, *J. Phys. Chem. B*, 2004, **108**, 3548-3562.
52. C. Hirose, N. Akamatsu and K. Domen, *Appl. Spectrosc.*, 1992, **46**, 1051-1072.
53. J. Löbau and K. Wolfrum, *J. Opt. Soc. Am. B*, 1997, **14**, 2505-2512.
54. C. Ohe, H. Kamijo, M. Arai, M. Adachi, H. Miyazawa, K. Itoh and T. Seki, *J. Phys. Chem. C*, 2008, **112**, 172-181.
55. B. Stuart, *Infrared spectroscopy fundamentals and applications*, J. Wiley, Chichester, Eng.; Hoboken, N.J., 2004.
56. E. H. Wong, R. Rajoo, T. B. Lim and Y.-W. Mai, *IEEE Transactions on Components and Packaging Technologies*, 2005, **28**, 862-868.

RSC Advances Accepted Manuscript

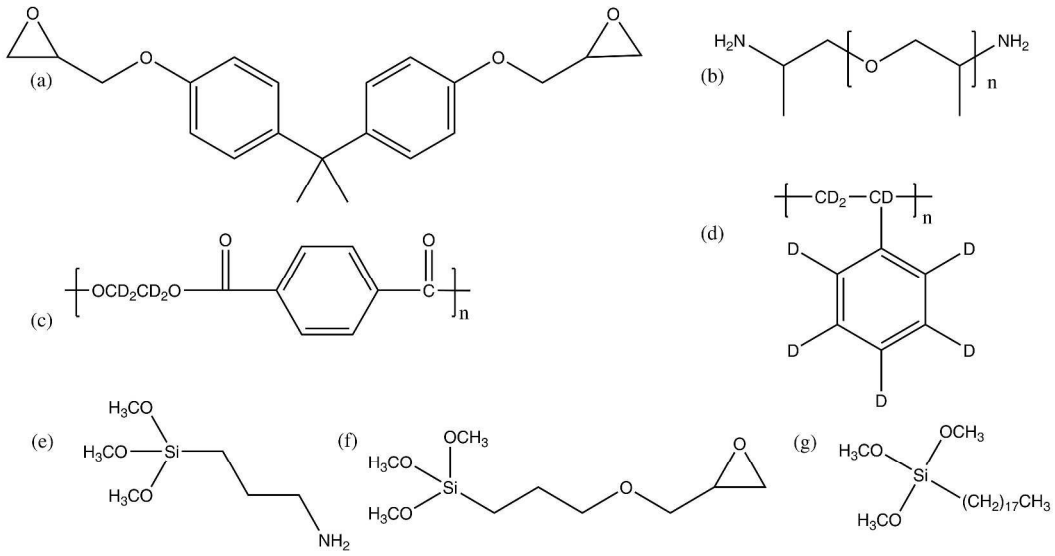

Figure 1: Chemicals used in the experiment: (a) bisphenol A diglycidyl ether (BADGE), (b) poly(oxypropylenediamine), (c) poly(ethylene terephthalate) with aliphatic chain deuterated (d4-PET), (d) deuterated polystyrene (d8-PS), (e) (3-Aminopropyl)trimethoxysilane (ATMS), (f) (3-glycidoxypropyl) trimethoxysilane (GPS), and (g) octadecyltrimethoxysilane (OTMS).

RSC Advances Accepted Manuscript

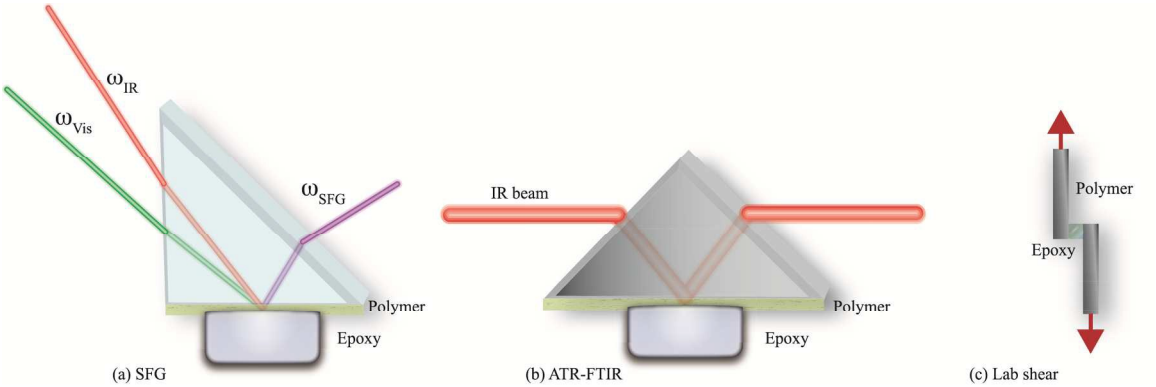

Figure 2: (a) SFG, (b) ATR-FTIR, and (c) lap shear experimental geometry utilized to study the epoxy buried interfaces.

RSC Advances Accepted Manuscript

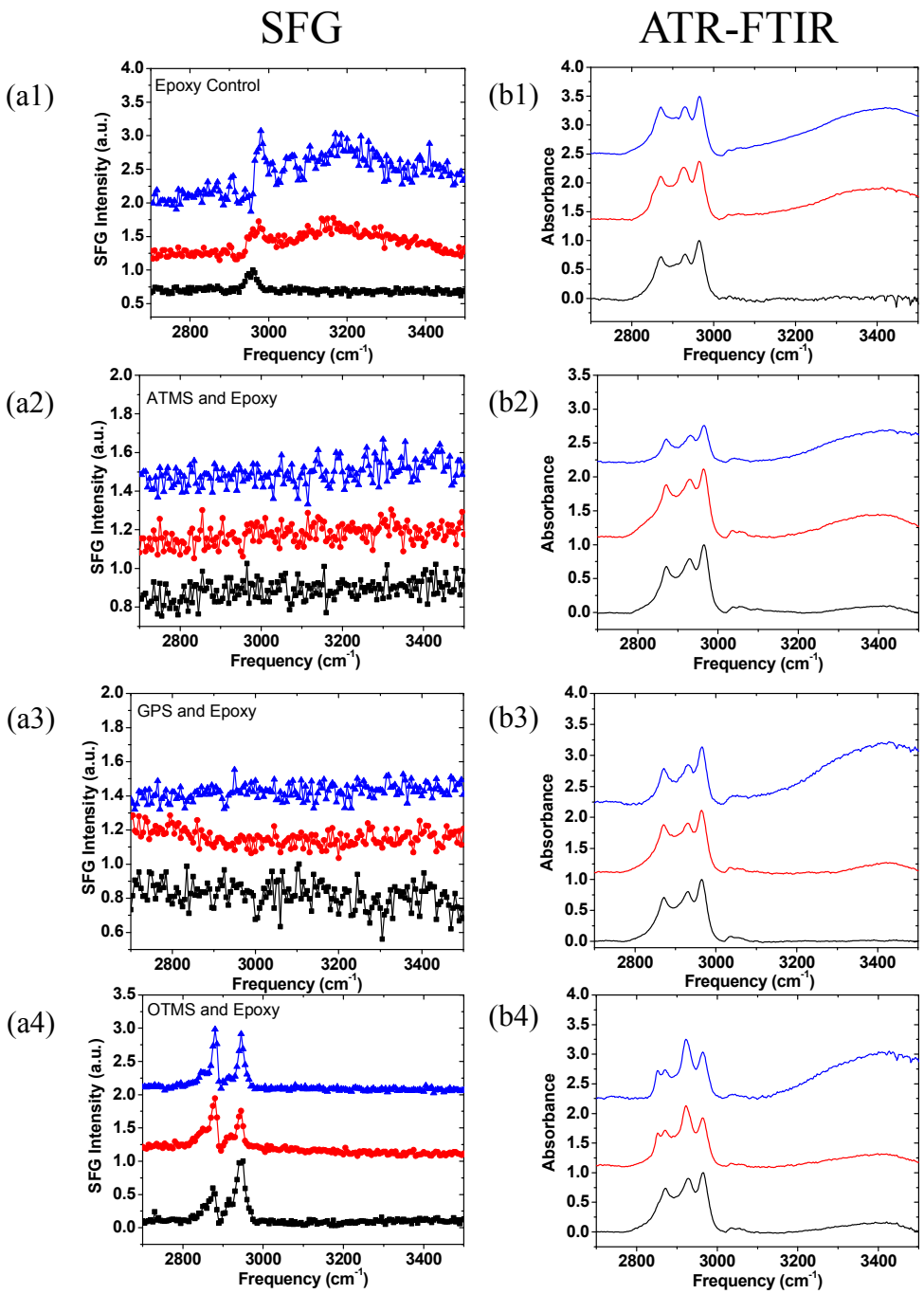

Figure 3: (a) SFG and (b) ATR-FTIR spectra collected from the interfaces between dPET and epoxy (1) without silane added to the epoxy, (2) with 1.5% ATMS in epoxy, (3) with 1.5 % GPS in epoxy, and (4) with 1.5% OTMS in epoxy. Black (bottom) spectra are collected at time zero, red (middle) spectra are collected after 24 hours hygrothermal treatment, and blue (top) spectra are collected after 48 hours hygrothermal treatment.

RSC Advances Accepted Manuscript

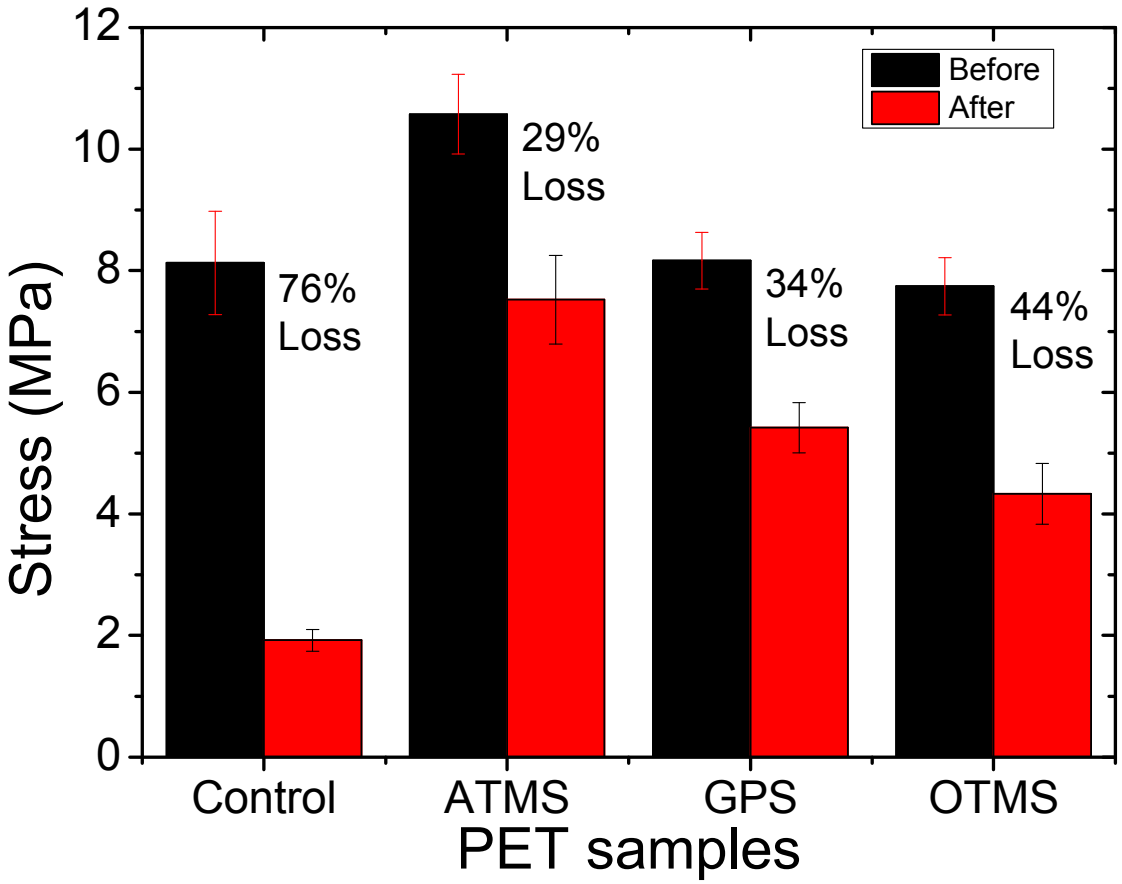

Figure 4: Adhesion testing results of dPET/epoxy interfaces with and without silane in epoxy. Adhesion strength is calculated by dividing the maximum adhesion force by the contact area. The black bar is before hygrothermal aging and the red bar is after 24 hours of aging. The error bars are the standard deviations.

RSC Advances Accepted Manuscript

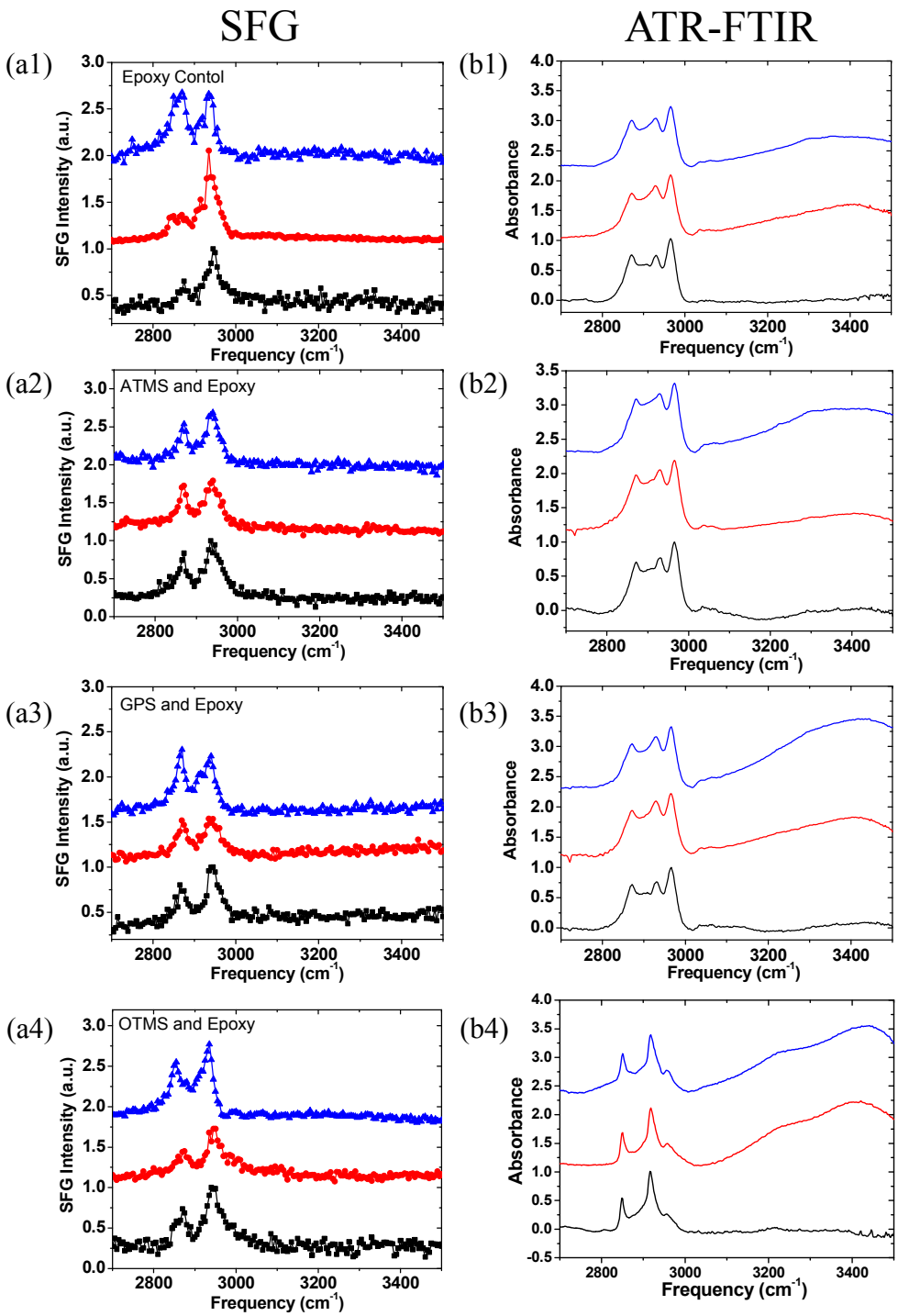

Figure 5: (a) SFG and (b) ATR-FTIR spectra collected from the interfaces between dPS and epoxy (1) without silane added to epoxy (2) with 1.5% ATMS added to epoxy, (3) with 1.5% GPS added to epoxy, and (4) with 1.5% OTMS added to epoxy. Black (bottom) spectra are collected at time zero, red (middle) spectra are collected after 24 hours hygrothermal treatment, and blue (top) spectra are collected after 48 hours hygrothermal treatment.

RSC Advances Accepted Manuscript

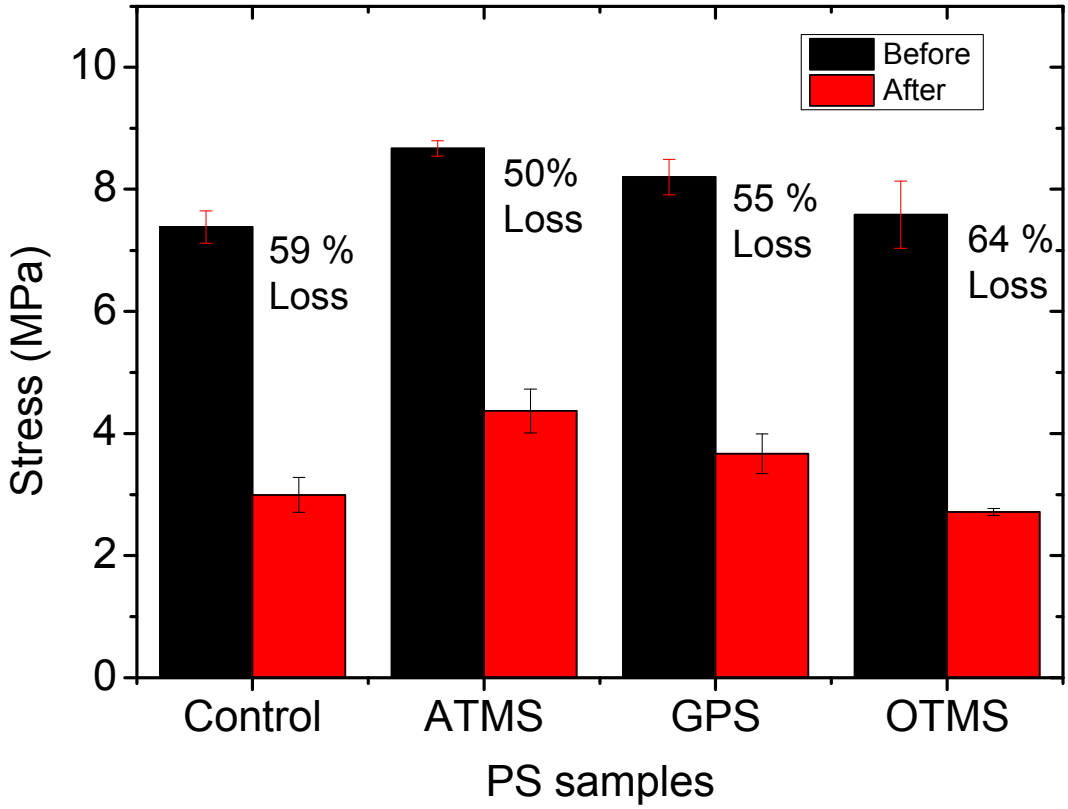

Figure 6: Adhesion testing results of dPS/epoxy interfaces with and without silane in epoxy. The black bar is before hygrothermal aging and the red bar is after 24 hours of aging. The error bars are the standard deviations.

RSC Advances Accepted Manuscript

Table of Contents

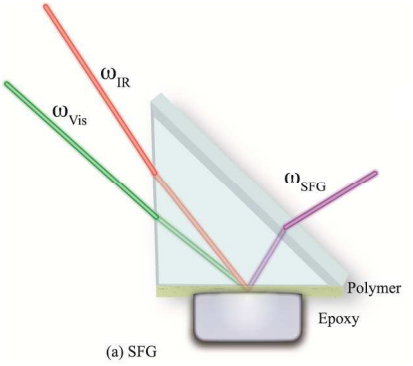

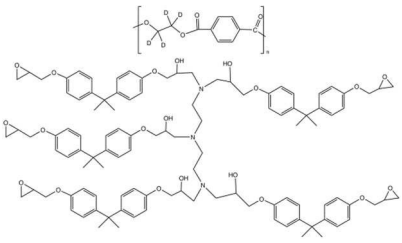

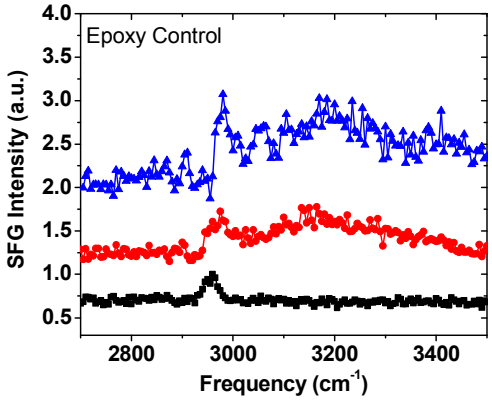

RSC Advances Accepted Manuscript